Faraday Wave Patterns on a Triangular Cell Network

Franklin Peña-Polo, Iván Sánchez and Leonardo Di G. Sigalotti

Abstract We present experimental observations of the Faraday instability when an air/water interface is split over a network of small triangular cells for exciting frequencies in the range $10 \leq f \leq 30$ Hz. Just above the threshold for instability, waves appear on the water surfaces within all individual cells. After a transient state, adjacent cells progressively synchronize and self-organize to produce a regular pattern covering the whole grid. Collective cell behaviour is seen to lead to four different patterns depending on the forcing frequency range. Beyond $\approx$28 Hz, adjacent cells no longer interact as the vibration wavelength becomes smaller than half the altitudes of the triangular cells and so the waves remain constrained within individual cells in the form of localized harmonic oscillons.

1 Introduction

When a close receptacle containing liquid is submitted to vertical vibrations, a pattern of non-linear standing waves is often observed at the surface of the liquid. These waves, known as Faraday waves (Faraday 1831), are parametrically excited when the vertical vibrations exceed a critical frequency f_c, or critical acceleration Γ_c. The acceleration Γ is defined according to the relation $\Gamma = A\omega^2$, where A is the excitation amplitude and $\omega (=2\pi f)$ is the circular frequency. Faraday (1831) realized that these waves are sub-harmonic because they oscillate at half of the harmonic

F. Peña-Polo (✉) · I. Sánchez · L. Di G. Sigalotti
Centro de Física, Instituto Venezolano de Investigaciones Científicas, IVIC, Apartado Postal 20632, Caracas 1020-A, Venezuela
e-mail: franklin.pena@gmail.com

I. Sánchez
e-mail: ivanjo@gmail.com

L. Di G. Sigalotti
e-mail: leonardo.sigalotti@gmail.com

L. Di G. Sigalotti et al. (eds.), *Computational and Experimental Fluid Mechanics with Applications to Physics, Engineering and the Environment*, Environmental Science and Engineering,
DOI:10.1007/978-3-319-00191-3_22,

excitation frequency. Modern experiments of single- and two-frequency forcing have revealed that not only spatially regular patterns of parallel lines, squares, circles, and hexagons may form but also many more complex symmetries such as quasi-patterns, superlattice patterns, and oscillons (Douady 1990; Edwards and Fauve 1994; Binks and van der Water 1997; Kudrolli et al. 1998; Arbell and Fineberg 2000a,b; Porter and Silber 2002; Westra et al. 2003).

Understanding the types of patterns that form is challenging. The threshold for instability and the observed patterns depend on the viscosity and surface tension of the fluid, the acceleration Γ, and the shape and size of the vessel. The full mathematical description of the problem involves the Navier-Stokes equations in a domain with a free surface, and the excitation makes the problem non-autonomous. In mathematics, a non-autonomous system is a system of ordinary differential equations which explicitly depends on the independent variable. In this case, non-autonomicity results from the external forcing that influences the fluid parameters when the oscillating behaviour initiates. On the other hand, the mechanisms of pattern selection have been investigated using the tools of symmetry and bifurcation theory (Silber et al. 2000; Rucklidge et al. 2003; Skeldon and Guidoboni 2007). The linear theory of this instability has been developed by Benjamin and Ursell (1954), who showed that the problem can be reduced to a set of Mathieu oscillators. However, the analysis relies on the potential flow approximation which is restricted to inviscid fluids only. If the instability is generated in a viscous liquid some mechanical energy is dissipated. These effects are usually treated by adding a heuristic damping in the Mathieu equation (Landau and Lifshitz 1987), which is proportional to the kinematic viscosity ν. The inclusion of such a term has been successively used in a number of linear analyses Müller (1993); Kumar and Tuckerman (1994); Kumar (1996) and Perlin and Schultz (2000). However, this approximation ignores viscous boundary layers along the vessel walls and beneath the surface, where additional dissipation occurs.

The most advanced theoretical investigation of the stability problem is fully numerical, which renders a physical understanding difficult Kumar and Tuckerman (1994). An analytic expression for the onset of sub-harmonic Faraday waves was obtained by Müller et al. (1997), which is applicable to a wide frequency range covering both shallow gravity and deep capillary waves. While this analysis is applicable in the limit of weak dissipation, an analytic treatment in the opposite limit was undertaken by Cerda and Tirapegui (1997). The linear aspects of the Faraday instability since Benjamin and Ursell (1954) were revisited by Müller (1998). It was not until very recently that the first numerical simulations of the dynamics of Faraday waves started to appear in the literature Périnet et al. (2009, 2012), involving the full solution of the Navier-Stokes equations in three-space dimensions coupled to a front-tracking method for resolving the free surface. In particular, these simulations have reproduced the square and hexagonal patterns seen in Kityk et al. (2005, 2009) with the same physical parameters. The hexagonal pattern was seen to be succeeded by recurrent alternation between quasi-hexagonal and beaded striped patterns.

In spite of recent progress, most work on Faraday waves assume that either the liquid bath has infinite extent or that the liquid surface is perfectly flat at the edge of the lateral walls where no-slip boundary conditions hold, which is unrealistic for

experiments where the meniscus dynamics is important (Douady 1990). In general, as the system is shaken, the effective gravitational acceleration varies, making the meniscus length to become alternately large and small. In order to preserve the fluid mass, surface waves are emitted from the sidewalls of the vessel at the driving frequency f. Viscous dissipation is the primary cause for damping of these capillary waves.

In containers of small size there exists a strong coupling between the capillary waves generated by the meniscus and the Faraday waves, where the former extend all over the liquid surface. Recent experimental observations with cylindrical vessels of small diameters indicate that an increase of the Γ_c threshold is required for exciting Faraday waves in such small recipients Nguyem Thu Lam and Caps (2011). As previously for the viscosity, the addition of a phenomenological damping term, proportional to the thickness of the boundary layer, to the linear theory for modelling the viscous dissipation due to meniscus waves has successfully reproduced the experimental measurements of Γ_c for instability (Nguyem Thu Lam and Caps 2011).

Alternatively to experiments with single small containers, the formation of regular patterns has also been observed over a square network of centimeter-sized cells (Delon et al. 2010). After a transient state, just above the Faraday threshold, adjacent cells synchronize to form regular square lattices over the entire network, whose orientation with respect to the grid depends on the exciting frequency range. In this chapter, we extend these experimental observations to the case of an isometric grid consisting of equilateral triangular cells and study the effects of this geometry on the collective cell behaviour.

2 Experimental Set-Up

The experimental set-up consists of a transparent Plexiglas vessel with a base size of $15 \times 15\,\mathrm{cm}^2$ and 15 cm high, containing on its bottom plate a vinyl grid consisting of 60 equilateral triangular cells of sides 25 mm and depth 15 mm each. The cells are filled with coloured distilled water up to a height of 7 mm, and placed on an electromagnetic shaker which produces a clean vertical acceleration waveform. Small holes (of diameter 0.5 mm) have been drilled at the bottom of each cell to ensure equality of the fluid level in all cells. Fluid motion into these holes is prevented by the viscosity of the fluid and the low frequencies of oscillation, typically of a few Hz.

The vessel acceleration, which is the relevant bifurcation parameter, is measured by a piezoelectric accelerometer fixed onto the shaker table, receiving an oscillating voltage. The signal from the accelerometer is acquired using a multifunctional data acquisition board and processed by a host computer, where a software is run to give the oscillation amplitude A in millimeters and the frequency f in Hz from the maximum acceleration Γ normalized to the gravitational acceleration g_0 ($= 9.81\,\mathrm{m\ s}^{-1}$). For pattern visualization the Plexiglas vessel is illuminated from above with white light using a pack of four halogen bulbs of 50 Watts each. The

bulbs were placed at a height of 80 cm from the Plexiglas vessel and turned on only during video recording for not more than 20 s in order to avoid alterations of the density, viscosity, and surface tension of water due to heating. At such height, the halogen bulbs will transmit an average heat power to the water surface of about 10 W, which may produce a temperature increase of 1°C only after 100 s of exposition. A CCD camera PL-B742 is used to observe the pattern from the top, and a second CCD camera (PL-B771) is positioned in front of one side of the vessel, tilted by an angle varied between 0 and 45° with respect to a plane perpendicular to the wall of the recipient, to record lateral and perspective views of the system. Pattern photographs from the top were also taken with a NIKON D60 digital SLR camera for presentation purposes. We varied the excitation frequency in the range between 10 and 30 Hz. For frequencies below ≈10 Hz, it is the maximum peak elevation which prevents the shaker from reaching the threshold acceleration Γ_c. Given the small size of the cells, the interaction between the meniscus and the Faraday waves are expected to have a stabilizing effect on the air/liquid interfaces (Nguyem Thu Lam and Caps 2011), thereby rising the instability threshold above the value required for non-confined liquids.

3 Observed Patterns

In a network of interconnected cells of small size, the relative effect of the numerous capillary menisci at the cell walls is an important factor. Due to the external forcing, the characteristic height of the menisci evolves according to $h = [\sigma/\rho g(t)]^{1/2}$ (Douady 1990), where σ is the surface tension of the liquid, ρ is its density, and $g(t)$ is the temporal modulation of gravity. This modification of the meniscus height leads to the generation of capillary waves, which dissipate by viscous shear and interact with the Faraday waves, excited sub-harmonically. This produces a stabilizing effect on the free surface so that more energy is required to excite Faraday waves than in large-recipient or non-confined fluids.

Just above ≈10 Hz, the wavelength of the forcing oscillations becomes smaller than the size of the cells, and after a transient state, adjacent cells progressively synchronize to form a regular pattern over the whole grid. Figure 1 shows top view photographs of the grid when bumps of fluid higher than the depth of the cells form at their intersections at $f = 10$ Hz and $\Gamma \approx 1.12 g_0$. If the driving force is maintained, the same pattern is recurrently repeated with periodic peak alternation occurring at the network scale along the horizontal direction every half a period as shown by the two images of Fig. 1. In this case, all adjacent cells collaborate synchronously to form a well-defined pattern by sharing nearly all of their liquid content into the emerging bumps. Some of them eventually pinch off at their ends and some liquid may be exchanged between adjacent cells. A similar collective behaviour was observed for higher exciting frequencies in the interval $10 \leq f \leq 14$ Hz. In particular, Fig. 2 displays a perspective view of this mode for $f = 12$ Hz. Synchronization is due to interacting cell waves converging at grid nodes as shown on the top left of Fig. 3.

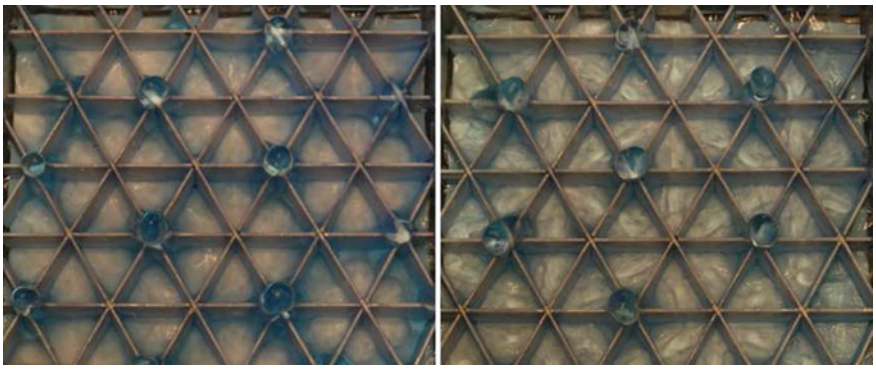

Fig. 1 *Top* view images of the resulting pattern at $f = 10\,\text{Hz}$. Liquid bumps appear at grid nodes at the dual vertical and triple horizontal network scale. Waves inside adjacent cells interact for a global synchronization with alternation of the peak positions every half a period as seen by comparing the two images

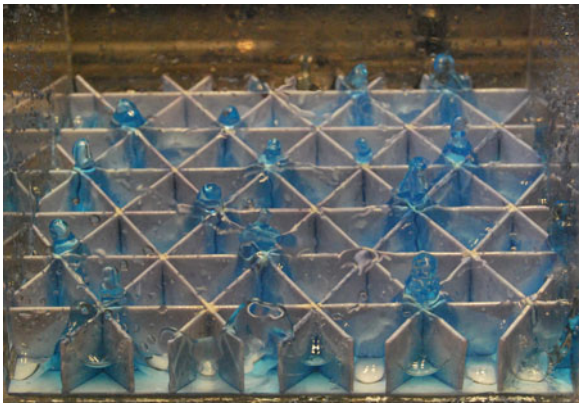

Fig. 2 *Perspective* view showing the bumps forming at grid intersections when a forcing frequency of 12 Hz is applied. This mode is the same of that in Fig. 1, except that at this frequency the nodal bump distribution looks a bit more irregular

Note that six cells arranged in a regular hexagon contribute to each bump in the network.

We have observed three more modes of synchronized collective behaviour depending on the frequency range as shown schematically in Fig. 3. For $15 \leq f \leq 17\,\text{Hz}$, the liquid bumps form at the edges of adjacent cells (top right), with no peaks appearing on grid nodes. This pattern arises because waves inside four adjacent cells interact at their common edges. In this case, the four contributing cells form a larger triangle. For $18 \leq f \leq 20\,\text{Hz}$, the patterning consists of bumps appearing again at cell edges (bottom left). However, this time only two adjacent cells are allowed to contribute and their union forms a rhombus. A top view photograph of this mode is

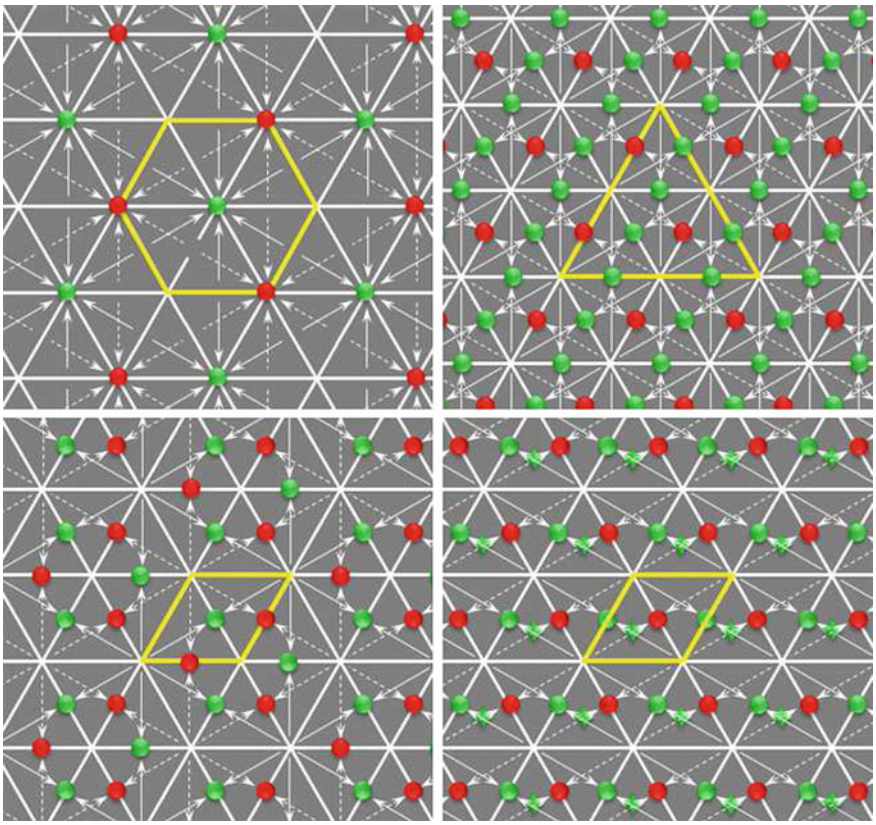

Fig. 3 Schematic of the four patterns observed according to the exciting frequency range: (i) $10 \leq f \leq 14\,\text{Hz}$ (*top left*), (ii) $15 \leq f \leq 17\,\text{Hz}$ (*top right*), (iii) $18 \leq f \leq 20\,\text{Hz}$ (*bottom left*), and (iv) $21 \leq f \leq 28\,\text{Hz}$ (*bottom right*). Alternation of the patterns is shown up by *green* and *red dots*, which mark the position of bumps at the beginning of and at half a period, respectively. The *arrows* indicate wave interaction between adjacent cells for one pattern (*continuous*) and its alternating counterpart (*dashed*). The *yellow* figures enclose the adjacent cells that work collectively

displayed in Fig. 4 at $f = 19\,\text{Hz}$ and $\Gamma \approx 2.38 g_0$. The two images are separated in time by half a period. Occasionally, some bumps may appear at grid nodes. For $21 \leq f \leq 28\,\text{Hz}$, peaks form synchronously at cell centres and edges owing to wave interaction between two adjacent cells (bottom right of Fig. 3). At such frequencies only part of the liquid inside a cell is shared with its neighbour, while the other part remains trapped within the cell to form a localized harmonic bump.

Beyond $\approx$28 Hz, the wavelength of the driving oscillations becomes smaller than half the triangular cell altitudes and so collective behaviour is no longer seen. The waves appear within each individual cell without interaction. The resulting pattern consists of localized harmonic oscillons forming at approximately the centre of each

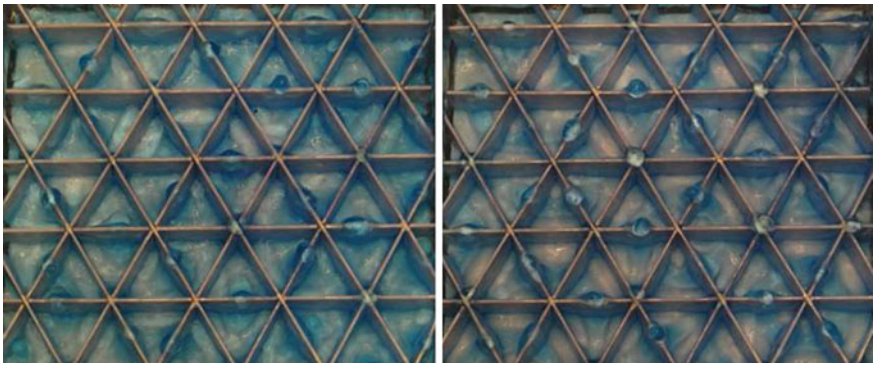

Fig. 4 *Top* view images of the observed pattern at $f = 19\,\text{Hz}$. Liquid peaks appear at the edges between adjacent cells. Occasionally some bumps may form at grid nodes. The alternation of the bump positions is not easily discerned from the two images

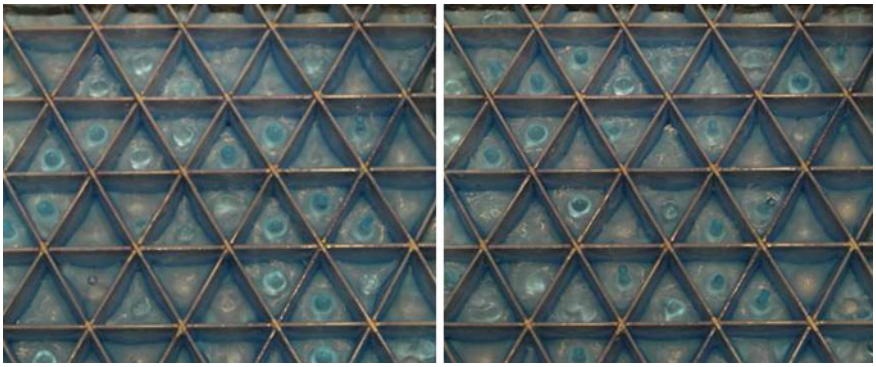

Fig. 5 Example of non-collective behaviour at $f = 30\,\text{Hz}$. At this frequency the waves remain constrained within each individual cell without interaction. The pattern consists of localized harmonic oscillons at the centre of cells

cell as shown in Fig. 5 at $f = 30\,\text{Hz}$ ($\Gamma \approx 2.45 g_0$). Note that the size of the peaks is irregular and that no peaks are produced within some cells.

4 Conclusion

We have presented experimental observations of the Faraday instability on a network of triangular cells. For exciting frequencies between 10 and 28 Hz, we have observed four different mode patterns. Depending on the frequency range, collective cell behaviour may results in symmetric patterns of liquid bumps, forming either at

grid nodes or at cell edges. Above ≈28 Hz, no collective behaviour is observed and temporally harmonic oscillons form at the centres of individual cells.

In previous experiments on a network of square cells, the liquid bumps formed square lattices at frequencies between 10 and 16 Hz due to diagonal wave interaction between adjacent cells (Delon et al. 2010). Evidently, changing the grid geometry from square to triangular not only adds an extra degree of freedom for wave interaction (due to the three altitudes in a triangular cell against the two diagonals in a square cell), but also doubles the number of patterns that forms along with the frequency range for which collective cell behaviour is observed.

References

Arbell H, Fineberg J (2000a) Two-mode rhomboidal states in driven surface waves. Phys Rev Lett 84:654–657

Arbell H, Fineberg J (2000b) Temporally harmonic oscillons in Newtonian fluids. Phys Rev Lett 85:756–759

Benjamin TB, Ursell F (1954) The stability of the plane free surface of a liquid in vertical periodic motion. Proc R Soc Lond A 225:505–515

Binks D, van der Water W (1997) Nonlinear pattern formation of Faraday waves. Phys Rev Lett 78:4043–4046

Cerda E, Tirapegui E (1997) Faraday's instability for viscous fluids. Phys Rev Lett 78:859–862

Delon G, Terwagne D, Adami N, Bronfort A, Vandewalle N, Dorbolo S, Caps H (2010) Faraday instability on a network. Chaos 20:041103

Douady S (1990) Experimental study of the Faraday instability. J Fluid Mech 221:383–409

Edwards WS, Fauve S (1994) Patterns and quasi-patterns in the Faraday experiment. J Fluid Mech 278:123–148

Faraday M (1831) On a peculiar class of acoustical figures; and on certain forms assumed by a group of particles upon vibrating elastic surfaces. Philos Trans R Soc London 121:299–318

Kityk AV, Embs J, Mekhonoshin VV, Wagner C (2005) Spatiotemporal characterization of interfacial Faraday waves by means of a light absorption technique. Phys Rev E 72:036209

Kityk AV, Embs J, Mekhonoshin VV, Wagner C (2009) Erratum: Spatiotemporal characterization of interfacial Faraday waves by means of a light absorption technique. Phys Rev E 79:029902

Kudrolli A, Pier B, Gollub JP (1998) Superlattice patterns in surface waves. Physica D 123:99–111

Kumar K, Tuckerman LS (1994) Parametric instability of the interface between two fluids. J Fluid Mech 279:49–68

Kumar K (1996) Linear theory of Faraday instability in viscous liquids. Proc R Soc Lond A 452:1113–1126

Landau L, Lifshitz EM (1987) Fluid Mechanics. Pergamon Press, New York

Müller HW (1998) Linear aspects of the Faraday instability. In: Parisi J, Müller SC, Zimmermann W (eds) A perspective look at nonlinear media from physics to biology and social sciences. Lecture Notes in Physics, vol 503. Springer, Berlin, pp 45–60

Müller HW (1993) Periodic triangular patterns in the Faraday experiment. Phys Rev Lett 71:3287–3290

Müller HW, Wittmer H, Wagner C, Albers J, Knorr K (1997) Analytic stability theory for Faraday waves and the observation of the harmonic surface response. Phys Rev Lett 78:2357–2360

Nguyem Thu Lam KD, Caps H (2011) Effect of capillary meniscus on the Faraday instability threshold. Eur Phys J E 34:112–116

Périnet N, Juric D, Tuckerman LS (2009) Numerical simulation of Faraday waves. J Fluid Mech 635:1–26

Périnet N, Juric D, Tuckerman LS (2012) Alternating hexagonal and striped patterns in Faraday surface waves. Phys Rev Lett 109:164501
Perlin M, Schultz WW (2000) Capillary effects on surface waves. Annu Rev Fluid Mech 32:241–274
Porter J, Silber M (2002) Broken symmetries and pattern formation in two-frequency forced Faraday waves. Phys Rev Lett 89:084501
Rucklidge AM, Silber M, Fineberg J (2003) Secondary instabilities of hexagons: a bifurcation analysis of experimentally observed Faraday wave patterns. In: Buescu J, Castro SBSD, Dias APS, Labouriau IS (eds) Bifurcations, symmetry and patterns. Birkhauser, Basel, pp 101–114
Silber M, Topaz CM, Skeldon AC (2000) Two-frequency forced Faraday waves: weakly damped modes and pattern selection. Physica D 143:205–225
Skeldon AC, Guidoboni G (2007) Pattern selection for Faraday waves in an incompressible viscous fluid. SIAM J Appl Math 67:1064–1100
Westra M-T, Binks DJ, van der Water W (2003) Patterns of Faraday waves. J Fluid Mech 496:1–32